Journal of Thermal Analysis and Calorimetry (2020) 139:1731–1739
https://doi.org/10.1007/s10973-019-08639-1

Production and in situ transformation of hematite into magnetite from the thermal decomposition of iron nitrate or goethite mixed with biomass

Marluce Oliveira da Guarda Souza[1] · Marcos Vinicius Ribeiro dos Santos[1] · Lucas Malone Ferreira Castro[1] · Carine Pereira da Silva[1]

Received: 20 October 2018 / Accepted: 25 July 2019 / Published online: 5 August 2019

Abstract
Among the methods of obtaining hematite (α-Fe_2O_3), the thermal decomposition of goethite (α-FeOOH) or iron (III) nitrate ($Fe(NO_3)_3{\cdot}9H_2O$) is of special importance. These solids can be combined with other materials, thus altering the properties of the oxide obtained. The decomposition of goethite or nitrate mixture with biomass in an inert atmosphere yields hematite/carbonaceous material or magnetite/carbonaceous composites with different morphologies and crystallinities, as observed by scanning electron microscopy and X-ray diffraction, respectively. The transformation of hematite to magnetite occurs at 623 K (for biomass/nitrate mixture) and 723 K (for biomass/goethite mixture). The formation of magnetite is a consequence of the pyrolysis of biomass, which produces a reducing mixture, and the difference in the temperature for obtaining Fe_3O_4 for the two precursors was investigated by thermal analysis by observing the mass and energy variations at each stage.

Keywords Hematite · Thermal decomposition · Goethite · Iron nitrate · Mango seed

Introduction

Iron oxides are found in different forms, with different properties and applications, which are present in hexagonal or cubic anion arrangements [1–4]. The interstices of these structures are partially filled with Fe^{2+} or Fe^{3+} ions, predominantly in octahedral coordination (FeO_6), but tetrahedral coordination (FeO_4) is also present [1, 3]. Hematite and magnetite are among the most abundant iron oxides [3, 5].

Hematite, the main naturally occurring iron ore, is red in color, has the molecular formula α-Fe_2O_3, and has semiconductor properties [1, 3, 5]. It is weakly ferromagnetic at room temperature and becomes paramagnetic at temperatures above 956 K (Curie temperature) due to thermal agitation overcoming the magnetic alignment and antiferromagnetic at $\sim$ 260 K (Morin temperature, Tm) [1]. Hematite has a corundum-type structure, and it can also be indexed in the rhombohedral system, with minimum two formulas per unit cell. This solid can exhibit different morphologies, with hexagonal or rhombohedral plates being the most common [1–5].

Magnetite, another important iron ore, is black in color and is a mixed oxide of FeO and Fe_2O_3 with the molecular formula Fe_3O_4 [2, 3, 5]. Due to the presence of mixed valences, magnetite exhibits cubic crystal structure of an inverse spinel, containing Fe^{2+} ions and a fraction of Fe^{3+} ions in the octahedral sites and the remaining Fe^{3+} ions in the tetrahedral sites [1–3, 5]. Magnetite shows ferromagnetic behavior due to the presence of Fe^{2+} ions, because the Fe^{3+} ions are equally divided among the octahedral and tetrahedral sites and therefore do not produce a net magnetic moment [1, 3]. Magnetite exists in different morphologies like polyhedra, flakes, spheres, and cubes, depending on the method of preparation [1, 3].

One method to obtain hematite is the thermal decomposition of goethite (α-FeOOH), an antiferromagnetic mineral that belongs to the iron oxide–hydroxide group and

✉ Marluce Oliveira da Guarda Souza
mosouza@uneb.br

[1] State University of Bahia, Silveira Martins Street 2555, Cabula, Salvador, BA 41.195.001, Brazil

is stable at room temperature [1–10]. The structure of this solid is orthorhombic, containing many Fe^{3+} ions coordinated by three O^{2-} anions and three OH^{-}, thereby forming an octahedron [1, 3, 5, 6]. Goethite can be synthesized by precipitation [3, 5].

The precipitation method involves the formation of a precipitate starting from supersaturation of a solution, usually aqueous, by evaporating the solvent or adding components that decrease solubility, for instance, by changing the pH. This process is crucial for the control of the solid morphology through nucleation, growth, and aggregation, or the adsorption of impurities [5].

Nucleation involves a combination of ions in solution that form small crystals that in turn give rise to particles of the precipitate. Growth corresponds to an increase in the size of the crystals formed. In these two steps, the particle size of the solid can be limited by controlling the variables such as pH, temperature, and nature of the precursor (chloride, sulfate, and nitrate) [5].

During the precipitation of iron salts in the presence of hydroxides or ammonium salts, $Fe(OH)_3$ species is formed, which is thermodynamically unstable (Eq. 1).

$$Fe(OH)_3 \rightleftarrows FeO(OH)(OH_2) \rightleftarrows \alpha\text{-}FeOOH + H_2O \quad (1)$$

There have been several studies regarding the thermal decomposition of goethite [4–10] of natural origin or synthetic (pure or mixed with other solids) to produce hematite. Heating α-FeOOH (iron III oxide–hydroxide), a gel with high surface area, to between 523 and 673 K, leads to the production of hematite (α-Fe_2O_3) by hydroxyl sheet removal, and some of the oxygen in strips is parallel to the *c*-axis to form water, as described by Eq. (2) [4–10].

$$2\alpha - FeOOH \rightarrow \alpha\text{-}Fe_2O_3 + H_2O \quad (2)$$

The reaction described by Eq. (2) is of great scientific and technological importance and has been the subject of several theoretical and experimental studies aimed at determining the influence of the process conditions on the properties of materials obtained after heat treatment [6–11]. For example, recent studies have demonstrated that gradual dehydroxylation under controlled conditions can produce efficient mesoporous adsorbents with surface sites containing the [FeOx(OH)] species [11].

By modifying the hematite production process of precipitation followed by thermal decomposition, it is possible to obtain magnetite with a high surface area. One example is the addition of acetate ions to the iron III oxide–hydroxide gel by adsorption, forming iron III hydroxyacetate, $Fe(CH_3COOH)_2(OH)$. Heating iron III hydroxyacetate in the temperature range 473 to 673 K in an inert atmosphere produces a gas mixture, formed especially by acetic acid, acetone, and carbon monoxide inside the solid, creating voids that contribute to the reduction of a fraction of the Fe^{3+} (Eq. 3) and the increase in the surface area [12–19].

$$Fe(CH_3COO^{-})_X(OH)_{3-x(s)} \rightarrow Fe_3O_{4(s)} \quad (3)$$

Hematite and magnetite can also be obtained by thermal decomposition of salts, for instance, pure iron nitrate (hematite form) or blended with a compound, the pyrolysis of which leads to the reducing of gases (magnetite form). The thermal decomposition of iron nitrate is a convenient technique for the production of highly homogeneous iron oxides with appropriate morphological characteristics for application in various fields [20, 21]. The initial thermal decomposition of iron (III) nitrate involves a complex mechanism consisting of dehydration, fusion evaporation/boiling, and simultaneous precipitation of $Fe(OH)(NO_3)_2$ as a result of the first hydrolysis event. The final product, hematite, is slowly formed as a result of the thermal dehydroxylation of FeOOH [20, 21].

The thermal decomposition of iron nitrate blends, goethite, and general iron ores with other materials such as biomass under an inert atmosphere produces reducing gases and may lead to the formation of magnetite [21–24]. Among the various forms of biomass used for this purpose is agro-industrial waste, specifically those produced from fruits used to obtain juices, jams, and sweets [25]. Mangoes in particular are rich in cellulose, hemicelluloses, and lignin, as are most biomasses of vegetal origin [25, 26].

Herein, the thermal decomposition of goethite/mango seed iron nitrate/mango seed mixtures was investigated using thermal analysis by observing mass and energy variations during each stage. The properties of the materials obtained after decomposition were characterized using various techniques.

Experimental

Preparation of iron oxides from goethite or iron (III) nitrate and biomass

Synthesis of goethite

Goethite was synthesized by precipitation using iron (III) nitrate. Iron (III) nitrate ($Fe(NO_3)_3{\cdot}9H_2O$) 1 mol L^{-1} and a precipitating agent (NH_4OH) 6 mol L^{-1} were simultaneously added to a beaker containing 500 mL of ultrapure water, resulting in a pH of 10, and the system was continuously agitated. The pH was maintained at 10 by adding small volumes of NH_4OH (25%) or nitric acid (10%). After the formation of the precipitate, the system was agitated for 30 min at room temperature, favoring the maturation of the crystals. Subsequently, the gel was separated by centrifugation at 250 rpm for 5 min and washed with ultrapure water

at 333 K for the removal of the nitrate ions. The number of washes was determined by nitrate test in the supernatant, performed by adding 1 mL of concentrated sulfuric acid (H_2SO_4) until there was no formation of the light brown ring that indicates the presence of nitrate ions. After washing, the gel was dried at 393 K for 12 h and the obtained solid was ground and sieved using an 80-mesh sieve [18].

Pretreatment of mango seed biomass

The biomass used was mango seeds obtained from a pulp factory located in the city of Salvador, BA. The seeds were washed with distilled water, sliced for the separation of the husk from the kernel, and dried (343 K, 48 h). Subsequently, they were ground in a knife mill and sieved in 80 mesh. The husk and kernel powders were mixed under mechanical agitation in the ratio of 1:2 (husk/kernel).

Preparation of goethite–biomass and iron nitrate–biomass mixtures

Physical mixtures were prepared with biomass (husk/kernel ½) and goethite or iron nitrate in the ratio of 1:1 (mass/mass). Biomass (10 g) was manually mixed with 10 g of goethite (or iron (III) nitrate) in an appropriate container, with successive agitations in all directions, for approximately 10 min at room temperature. In the case of mechanical mixture of solids, the possibility of synthesizing new materials with specific properties for a given application by using a simpler method that combines the desirable properties of each component was considered [27, 28]. Additionally, the mechanical mixture can guarantee correct dosage and homogenization [27, 28]. One great advantage of this method is the reduction of material and reagent use, as well as certain equipment, unlike the other procedures found in the literature.

Thermal decomposition of the goethite–biomass and iron nitrate–biomass mixtures

The goethite (or iron nitrate)–biomass mixture was heated to 473, 623, and 723 K using a muffle furnace with nitrogen (N_2) at the flow rate of 100 mL min^{-1} and heating rate of 283 K min^{-1} and maintained for 1 h after reaching the target temperature. The iron nitrate–biomass mixtures were heated under the same conditions.

Characterization of the samples

Characterization of the precursors

The precursors (goethite, nitrate, and mixtures) were characterized by thermal analysis (TG/DTA). The analyses were performed in Shimadzu TA-60 WS equipment at the heating rate of 283 min^{-1} under nitrogen flow (N_2) at the rate of 50 mL min^{-1} in the temperature range 298 to 1273 K. The mass used in each analysis was approximately 10 mg.

Characterization of the materials obtained after thermal decomposition of the mixtures

X-ray diffraction (XRD) X-ray diffraction analyses were performed using Shimadzu equipment model XRD-6000 with Cu Kα radiation (λ = 1.5418 Å). The samples were analyzed by the powder method and the experiments performed in the analysis 2θ interval of 10°–80°, with the scan speed of 2° min^{-1}. The results were compared with the International Center of Diffraction Data (ICDD-2001) database for identification of the crystal phases.

Scanning electron microscopy (SEM) SEM images were obtained with the JEOL electron microscope model JSM-T300 operating in the range 20 to 30 kV. The samples were placed on the surface of a brass cylinder of diameter 1 cm covered with a double-sided tape. Then, a 300-A carbon coating was formed.

Results and discussion

Thermal analysis of the precursors

To better understand the decomposition process of the mixtures (biomass–goethite or biomass–iron III nitrate), each precursor was initially analyzed individually.

Thermal analysis of goethite

The TGA and DTA curves of goethite (Fig. 1) indicated two mass loss processes, corresponding to the release of volatile matter from the sample in the temperature range 300 to 373 K, for which the percentage of mass lost was 11.70%. The DTA curve presents an endothermic peak associated with the same process, at the temperature of 343 K.

The second step of mass loss (5.06%), corresponding to dehydroxylation of the material between 383 and 673 K, can be initially associated with the formation of amorphous iron oxide, followed by the crystallization of hematite, indicating exothermic peaks at 509 K and 702 K in the DTA curve [18, 19].

Thermal analysis of iron nitrate

The thermal decomposition curves (TGA and DTA) of iron nitrate are shown in Fig. 2. Mass loss can be observed at

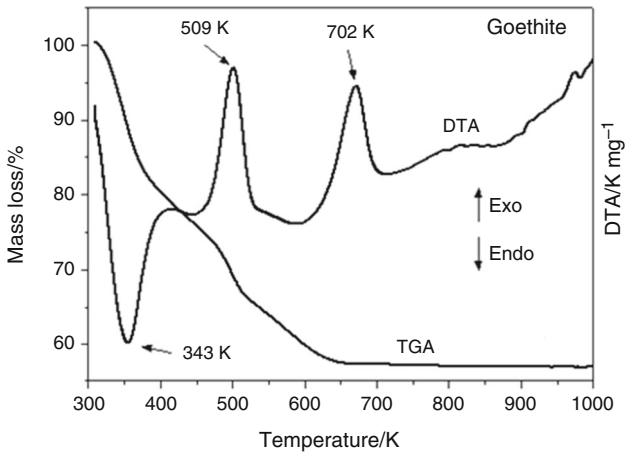

Fig. 1 TGA and DTA curves of goethite

temperatures below 373 K, with the total being 36.22%. Such processes are endothermic, as evidenced by the peaks in the DTA curve, at the temperatures 328 K and 366 K These were associated with the dehydroxylation and/or release of water, especially the physisorbed water in the material that, in addition to being hydrated, presents the very common property observed among most salts, the hygroscopic (water absorption) capacity [20]. The decomposition step in the range 383 to 473 K corresponds to the release of nitrate ions through the formation of nitric acid or nitrogen dioxide, with 21.88% mass loss. Such processes are endothermic, as evidenced by the peaks in the DTA curve, at the temperatures 402 K and 430 K. In the same stage, according to Muller et al., iron oxide starts forming from the temperature of 439 K [20]. However, crystallization of the hematite phase only occurs at higher temperatures, as evidenced by the exothermic peak with the maximum at 716 K [20, 21].

Thermal analysis of the biomass

Figure 3 indicates the three steps of mass loss characteristic of the biomass (mango seed) decomposition. The profile is similar to that reported in the literature for the thermal decomposition of certain lignocellulosic materials [29–33]. According to the literature [29], the first step of mass loss, between 300 and 373 K, can be associated with the loss of moisture (12.36%). In the next step, the degradation of cellulose and hemicelluloses is observed in the temperature range 379 to 668 K, with 56.47% of mass lost [31]. The end of the decomposition process of this material occurs with the degradation of lignin. Because of its high resistance, this occurs over a wider range of temperatures, 463 to 973 K, with 10.30% mass loss [31]. The DTA curve exhibits peaks associated with both endothermic and exothermic events. One endothermic peak is observed at the temperature of 338 K, corresponding to the loss of moisture observed in the TGA curve, and three exothermic peaks related to the decomposition of the main biomass components cellulose, hemicelluloses, and lignin are observed at the temperatures of 573, 614, and 679 K, respectively [33, 34].

Thermal analysis of the goethite–biomass mixtures

The thermogravimetric curves for the thermal decomposition (TGA/DTA) of the goethite/biomass mixture (Fig. 4) reveal four steps of mass loss. These thermal events are associated with the degradation of the main components of the mixture. At the first step, until 373 K, there is a loss in mass of 9.29% related to the volatile matter present in the material followed by an endothermic peak in the DTA curve (338 K). There is a second mass loss (8.16%) in the range 373 to 523 K related to dehydroxylation, with the release of the residual nitrate ions present in the sample and the beginning of the formation of an amorphous and

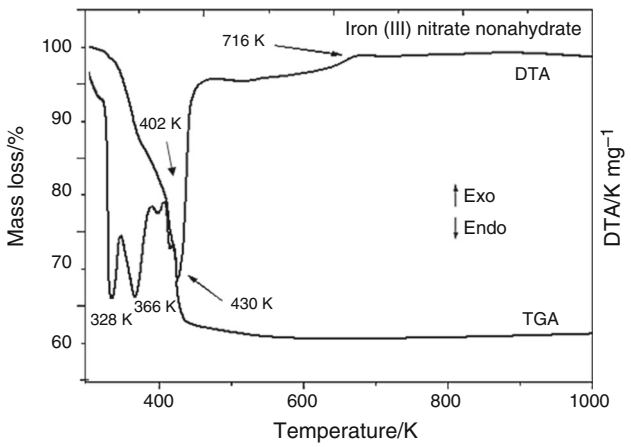

Fig. 2 TGA and DTA of iron (III) nitrate

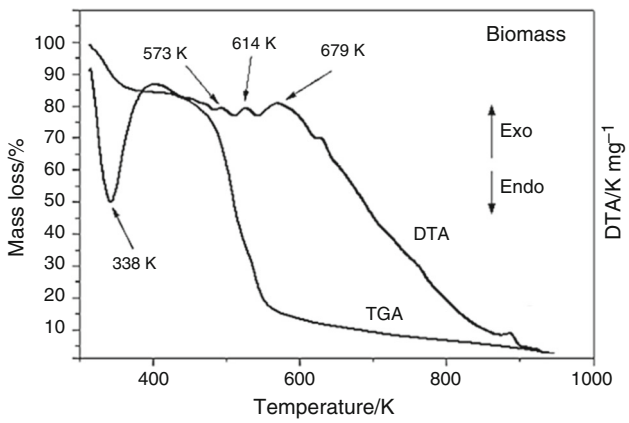

Fig. 3 TGA and DTA of biomass (mango seed)

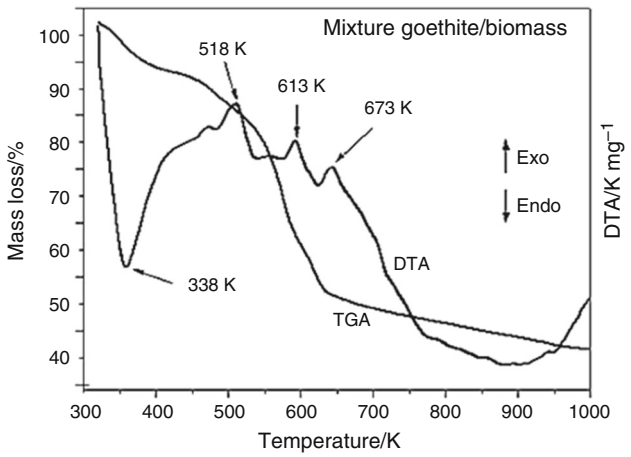

Fig. 4 TGA and DTA of goethite/biomass (mango seed) mixture

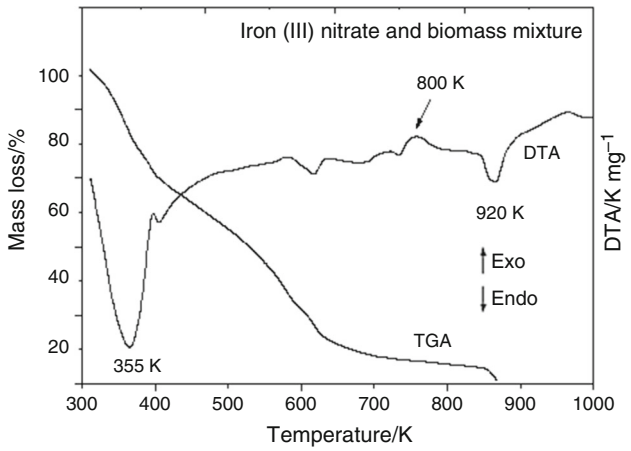

Fig. 5 TGA and DTA of iron (III) nitrate/biomass (mango seed) mixture

irregular structure of iron oxide and also the decomposition of the biomass components cellulose and hemicellulose, followed by an exothermic peak in the DTA curve with the maximum at 518 K. In the region of 533 to 623 K, the crystallization of iron oxide occurs simultaneously with the decomposition of cellulose and hemicelluloses and the start of the decomposition of lignin, with 34.33% mass loss. This causes the release of reducing gases, which may lead to the reduction of Fe(III) to Fe(II) ions with the formation of magnetite [21]. The last step corresponds to the end of the degradation of lignin in the range 623 to 1000 K, with 10.41% mass loss [33, 34]. In the range 533 to 1000 K, two exothermic peaks are observed in the DTA curve (613 and 673 K).

Thermal analysis of the iron (III) nitrate–biomass mixture

The profile of the thermogravimetric curve (Fig. 5) of the physical mixture of the mango seed and the iron nitrate indicated mass loss events characteristic of the thermal decomposition common to the precursor materials (biomass and iron nitrate). The first stage of decomposition occurred at the temperature of 373 K and can be attributed to the elimination of water and volatile matter from both the materials that compose the mixture, resulting in a total of 31.82% mass loss. In the range of 373 K to approximately 473 K, a mass loss of 23.66% was observed, which may be associated with the thermal decomposition of iron (III) nitrate simultaneous to those of the biomass components [21, 34]. The decomposition step in the range 493 to 653 K is associated with the decomposition of hemicelluloses from the biomass and the end of the decomposition of iron nitrate, with the mass loss being 12.17%. In this temperature range, the thermal decomposition of iron (III) nitrate leads to the formation of the corresponding iron oxide (hematite, α-Fe_2O_3), which can be reduced to magnetite (Fe_3O_4), since some gases and volatile compounds released during the decomposition of the biomass form a reducing atmosphere, as previously discussed [21, 34]. In this case, the resulting process is exothermic, as observed in the DTA curve in the temperature range 603 to 673 K. The last stage of decomposition occurs between 653 and 923 K and is associated with the thermal degradation of lignin with a mass loss of 7.35% [32, 33]. Therefore, in this temperature range, the release of reducing gases that may reduce magnetite to form metallic iron is still noticed, justifying the exothermic peak observed in the DTA curve with the maximum at 800 K. The mass loss observed is the result of the balance between the amount of gases released and that consumed during the reduction. The adsorption of methane (one of the produced gases) may also occur on the surface of the metallic iron [21, 34]. In this case, iron catalyzes the cracking process of methane, resulting in the formation of carbon, which is adsorbed on the surface. In a gaseous atmosphere enriched by carbon compounds, the iron is supersaturated with carbon, resulting in the formation of iron carbide, Fe_3C, as observed in a previous study [21]. The endothermic peak observed at 920 K in the DTA curve may be associated with the decomposition of Fe_3C, which is unstable, and upon heating at temperatures higher than 873 K, the formation of metallic iron and carbon (soot) may occur [21].

Materials obtained after the thermal treatment of the precursors

Goethite-based materials

X-ray diffraction According to the analyzed X-ray diffractograms of the samples obtained by heating the physical mixture of goethite/biomass (Fig. 6), heating at 473 K barely changed the profile in relation to that of the

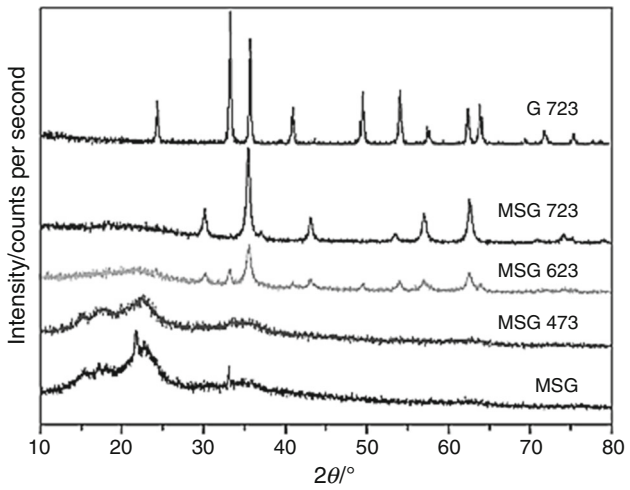

Fig. 6 XRD curves of composites mixture from goethite/biomass (mango seed)

unheated sample (MSG), which indicates the presence of cellulose corresponding to the peaks between 18° and 23° [35, 36], a fact that is better observed in the diffractogram of the biomass with no thermal treatment (JCPDS 2001).

The mixture profiles indicate that an increase in the treatment temperature to 623 K and 723 K led to the formation of two crystal structures different from that of iron oxide, revealing characteristic peaks of hematite (JCPDS 86-0550) and, predominantly, magnetite (JCPDS 19-0629), respectively. In addition, the phase present in the sample obtained after the thermal treatment of pure goethite is hematite. Based on these results, it can be inferred that the heating of the biomass/goethite mixture at 623 K leads to the formation of hematite, along with the commencement of the reduction to magnetite, where the reduction process is more efficient at 723 K, which corroborates with the results obtained from the thermal analysis (TGA/TDA) and the literature [21, 34].

Scanning electron microscopy According to the micrographs of the materials obtained after the thermal treatment of the mixture at different temperatures (Fig. 7), morphological changes are observed with the increase in the temperature. Such alterations are less visible in the sample heated at 473 K which still exhibits the presence of characteristic fibers of the biomass components (cellulose, hemicelluloses, and lignin), also observed in the micrograph of the material *in natura* [29]. These observations corroborate with the thermal analysis (TGA and DTA) results, since, at this temperature, there is no significant decomposition of the biomass components.

The most significant changes are observed in the images of the materials heated at 623 K and 723 K. These changes

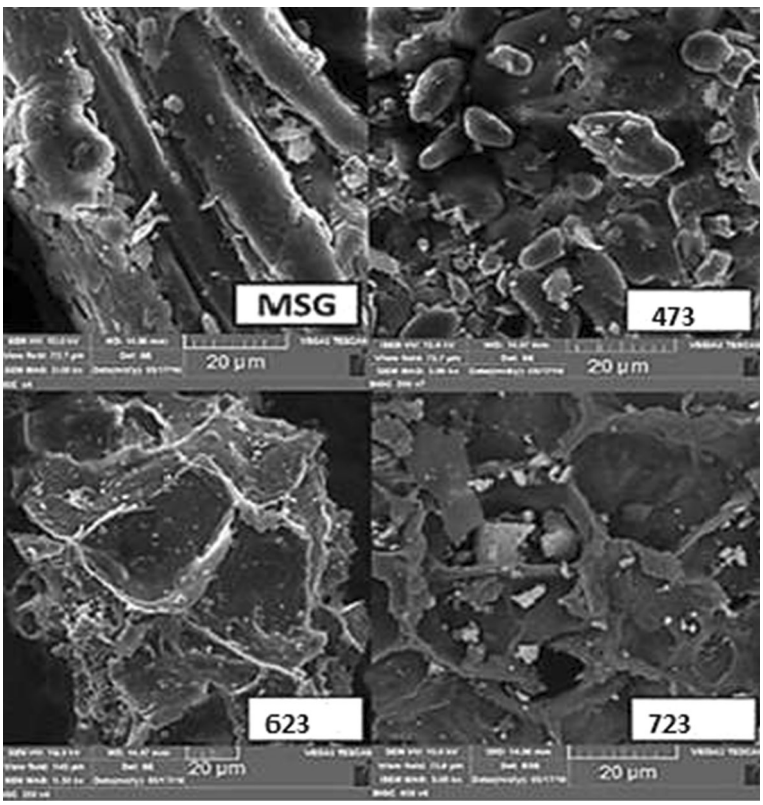

Fig. 7 SEM images of mixture goethite/biomass (mango seed) after thermal treatment

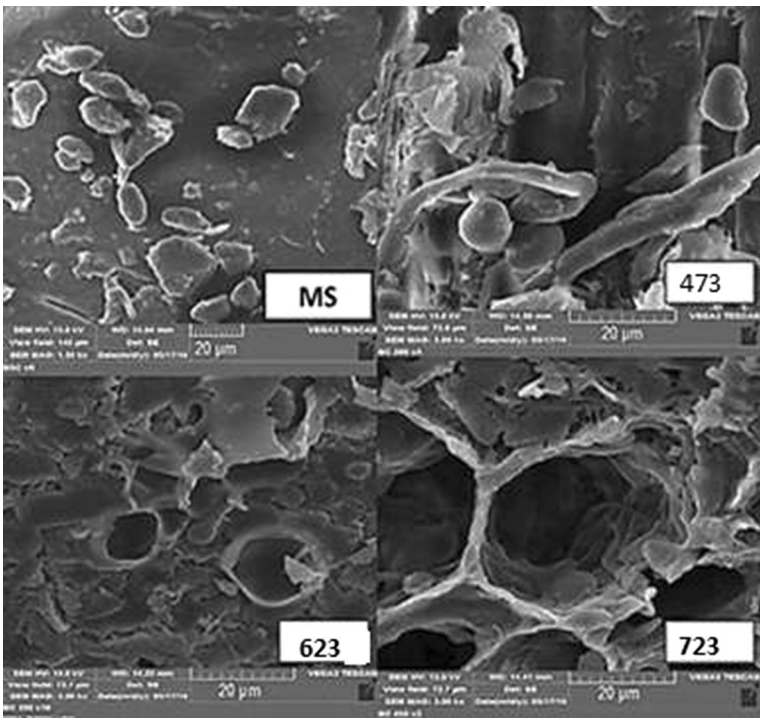

Fig. 8 SEM images of biomass (mango seed) after thermal treatment

are associated with the biomass decomposition process, especially involving cellulose and hemicellulose, which, according to the thermogravimetric analysis, are completely decomposed between 573 and 723 K. The micrographs of the two samples indicate small particles distributed in the carbonaceous matrix, which can be associated with the iron oxide formed above 623 K, according to the X-ray diffractograms.

The aspects discussed in the previous sections become more evident when comparing the micrographs of the mixtures after thermal treatment at the different temperatures (Fig. 7) with those of the pure biomass thermally treated under the same conditions (Fig. 8). The comparison reveals that the observed particles are iron oxides distributed in the carbonaceous matrix.

Iron nitrate-based materials

X-ray diffraction Figure 9 presents the diffraction profiles of the biomass–iron nitrate mixtures treated at different temperatures and the profile of pure nitrate after thermal treatment at 723 K (N723) to form the hematite phase, which is used as Ref. [21]. As observed, the mixtures MSN and MSN473 reveal amorphous diffraction profiles upon irradiation with X-rays. In addition, the samples obtained by thermal decomposition at 623 K and 723 K exhibit characteristic peaks of the magnetite phase, though the crystallinity is lower in relation to the samples MSN623 and MSN723, indicating that the nature of the precursor affects the crystallinity of the iron oxide formed.

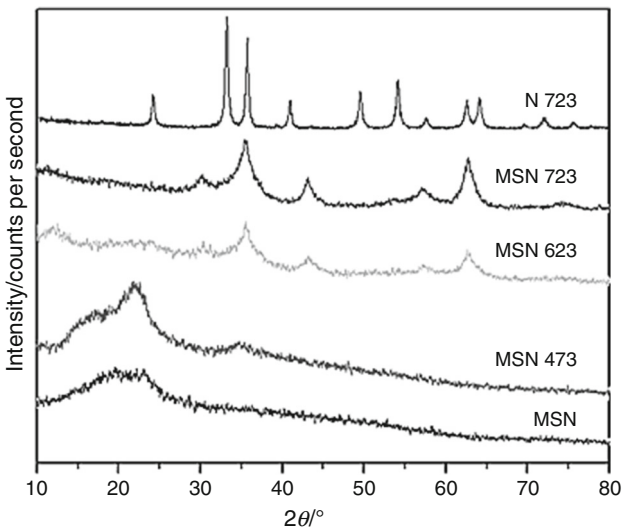

Fig. 9 XRD curves of composites mixture from iron nitrate/biomass (mango seed)

Scanning electron microscopy The microscopy images of the materials obtained by thermal treatment of the mixture formed by iron nitrate and mango seed indicated a completely different morphology than that observed in the pure biomass (Fig. 10). In this case, it was not possible to identify the lignocellulosic compositions of the samples MSN and MSN473. This corroborated with the absence of cellulose peaks in the diffractograms of these samples. The micrographs of the materials obtained after thermal treatments at 623 K and 723 K reveal the characteristic

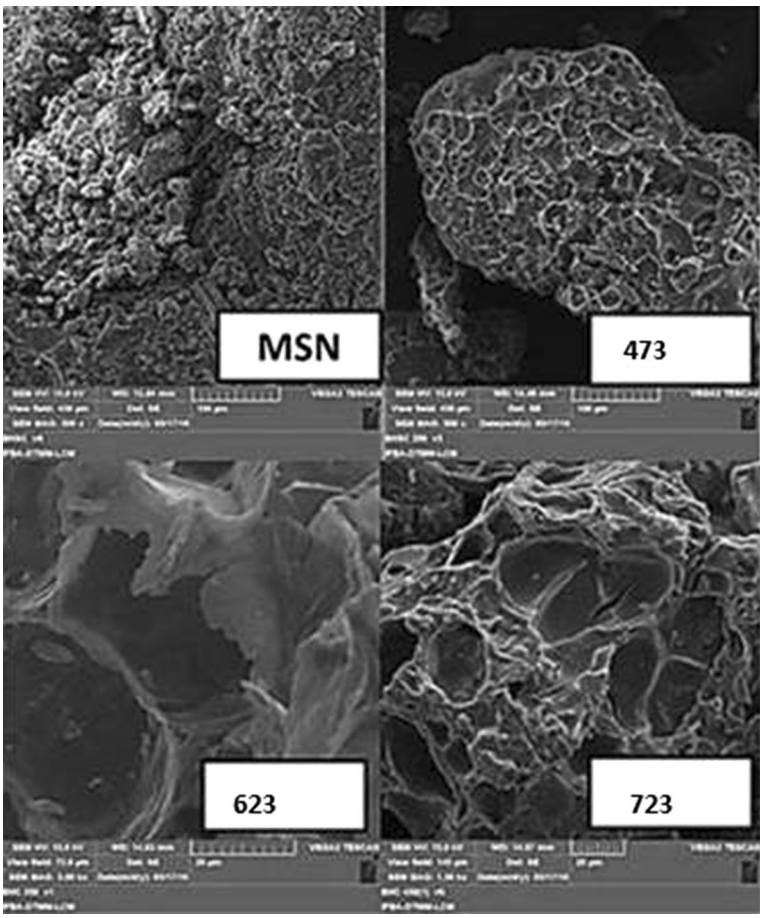

Fig. 10 SEM images of mixture formed by iron nitrate and mango seed after thermal treatment

morphologies of the carbonaceous material [21], where small crystals or particles of the amorphous iron oxide formed are distributed, in accordance with the X-ray diffraction results that suggest that the material formed at 623 K, as well as at 723 K, exhibits low crystallinity.

Conclusions

A mixture of iron oxide precursors (goethite or nitrate) with mango seeds (integument and nut 1/2) can modify the phase obtained by thermal decomposition of such precursors (hematite). At the temperature of 623 K, the formation of a mixture of hematite and magnetite is observed, while at 723 K, magnetite is the predominant phase. This modification is due to the reducing gas mixture formed during the decomposition of the biomass components cellulose, hemicelluloses, and lignin. The solids produced from the mixture of goethite and biomass are more crystalline than those obtained from the mixture of nitrate and biomass and reveal different morphologies. Such differences can be associated with the results observed in TGA/DTA thermal analysis.

Acknowledgements The authors would like to thank the Applied Chemistry Postgraduate Program (PGQA) Capes, Fapesb for the granted infrastructure and Capes for their financial support.

References

1. Silva MF, Pineda EAG, Bergamasco R. Aplicação de óxidos de ferro nanoestruturados como adsorventes e fotocatalisadores na remoção de poluentes de águas residuais. Quim Nova. 2015;38:393–8.
2. Zorzi JE, Perottoni CA, Cruz RCD. Determination of ferrous and ferric iron from total iron content and thermogravimetric analysis. J Therm Anal Calorim. 2018;136:1879–86.
3. Oliveira LCA, Fabris JD, Pereira MC. Óxidos de ferro e suas aplicações em processos catalíticos: uma revisão. Quim Nova. 2013;36:123–30.
4. Rocha VMDS, Pereira MDG, Teles LR, Souza MODG. Effect of copper on the photocatalytic activity of semiconductor-based titanium dioxide (anatase) and hematite (α-Fe_2O_3). Mater Sci Eng B Solid State Mater Adv Technol. 2014;185:13–20.
5. Cornell RM, Schwertmann U. The iron oxides: structure, properties, reactions, occurrences and uses. 2nd ed. Weinheim: Wiley-VCH Verlag GmbH & Co.KGaA; 2003.
6. Frost RL, Ding Z, Ruan HD. Thermal analysis of goethite: relevance to Australian indigenous art. J Therm Anal Calorim. 2003;71:783–97.
7. Liu H, Chen T, Frost RL. An overview of the role of goethite surfaces in the environment. Chemosphere. 2014;103:1–11.

8. Ruan H, Frost R, Kloprogge J, Duong L. Infrared spectroscopy of goethite dehydroxylation: III. FT-IR microscopy of in situ study of the thermal transformation of goethite to hematite. Spectrochim Acta Part A Mol Biomol Spectrosc. 2002;58:967–81.
9. Liu H, Chen T, Zou X, Qing C, Frost RL. Effect of Al content on the structure of Al-substituted goethite: a micro-Raman spectroscopic study. J Raman Spectrosc. 2013;44:1609–14.
10. Liu H, Chen T, Zou X, Qing C, Frost RL. Thermal treatment of natural goethite: thermal transformation and physical properties. Thermochim Acta. 2013;568:115–21.
11. Pinto PS, Lanza GD, Ardissonb JD, Lago RM. Controlled dehydration of $Fe(OH)_3$ to Fe_2O_3: developing mesopores with complexing iron species for the adsorption of β-lactam antibiotics. J Braz Chem Soc. 2019;30(2):310–7.
12. Júnior IL, Millet J-MM, Aouine M, do Carmo Rangel M. The role of vanadium on the properties of iron based catalysts for the water gas shift reaction. Appl Catal A Gen. 2005;283:91–8.
13. Rangel MC, Sassaki RM, Galembeck F. Effect of chromium on magnetite formation. Catal Lett. 1995;33:237–54.
14. Monteiro DS, Souza MOG. Thermal decomposition of precursors and iron oxide properties. J Therm Anal Calorim. 2016;123:955–63. https://doi.org/10.1007/s10973-015-4840-5.
15. Habibi MH, Kiani N. Preparation of single-phase α-Fe(III) oxide nanoparticles by thermal decomposition. Influence of the precursor on properties. J Therm Anal Calorim. 2013;112:573–7.
16. Malek TJ, Chaki SH, Tailor JP, Deshpande MP. Nonisothermal decomposition kinetics of pure and Mn-doped Fe_3O_4 nanoparticles. J Therm Anal Calorim. 2018;132:895–905.
17. Wang Y, Wang X, Hua X, Zhao C, Wang W. The reduction mechanism and kinetics of Fe_2O_3 by hydrogen for chemical-looping hydrogen generation. J Therm Anal Calorim. 2017;129:1831–8.
18. Souza MO da G, Quadro EB, Rangel M do C. Propriedades texturais e catalíticas de óxido de ferro contendo cromo e cobre. Quim Nova. 1998;21:428–33.
19. de Araujo GC, de Souza AO, Rangel M do C, Pinheiro EA. Efeito da temperatura no desempenho catalítico de óxidos de ferro contendo cobre e alumínio. Quim Nova. 2002;25:181–5.
20. Wieczorek-Ciurowa K, Kozak AJ. The thermal decomposition of $Fe(NO_3)_3{\cdot}9H_2O$. J Therm Anal Calorim. 1999;58:647–51.
21. Silva CP, dos Santos AV, Oliveira AS, Souza MO da G. Synthesis of composites and study of the thermal behavior of sugarcane bagasse/iron nitrate mixtures in different proportions. J Therm Anal Calorim. 2017;131:611–20.
22. Abd Rashid RZ, Mohd. Salleh H, Ani MH, Yunus NA, Akiyama T, Purwanto H. Reduction of low grade iron ore pellet using palm kernel shell. Renew Energy. 2014;63:617–23.
23. Luo S, Yi C, Zhou Y. Direct reduction of mixed biomass-Fe_2O_3 briquettes using biomass generated syngas. Renew Energy. 2011;36:3332–6.
24. Müller M, Villalba JC, Mariani FQ, Dalpasquale M, Lemos MZ, Gonzalez Huila MF, et al. Synthesis and characterization of iron oxide pigments through the method of the forced hydrolysis of inorganic salts. Dyes Pigments. 2015;120:271–8.
25. Asif A, Farooq U, Akram K, Hayat Z, Shafi A, Sarfraz F, et al. Therapeutic potentials of bioactive compounds from mango fruit wastes. Trends Food Sci Technol. 2016;53:102–12.
26. Correia LB, Fiuza RA, de Andrade RC, Andrade HMC. CO_2 capture on activated carbons derived from mango fruit (*Mangifera indica* L.) seed shells. J Therm Anal Calorim. 2018;131:579–86.
27. Jayamurugan P, Ponnuswamy V, Ashokan S, Jayaprakash R, Ashok N, Guna K, et al. DBSA doped polypyrrole blended with poly(4-styrenesulfonic acid) by mechanical mixing. Mater Sci. 2014;32:648–51.
28. Khalil I, Naaman A, Camilleri J. Investigation of a novel mechanically mixed mineral trioxide aggregate (MM-MTA^{TM}). Int Endod J. 2015;48:757–67.
29. Chen Z, Hu M, Zhu X, Guo D, Liu S, Hu Z, et al. Characteristics and kinetic study on pyrolysis of five lignocellulosic biomass via thermogravimetric analysis. Bioresour Technol. 2015;192:441–50.
30. Elizalde-González MP, Hernández-Montoya V. Characterization of mango pit as raw material in the preparation of activated carbon for wastewater treatment. Biochem Eng J. 2007;36:230–8.
31. Henrique MA, Silvério HA, Flauzino Neto WP, Pasquini D. Valorization of an agro-industrial waste, mango seed, by the extraction and characterization of its cellulose nanocrystals. J Environ Manag. 2013;121:202–9.
32. Souza FG, da Silva AM, de Oliveira GE, Costa RM, Fernandes ER, Pereira ED. Conducting and magnetic mango fibers. Ind Crops Prod. 2015;68:97–104.
33. Mallick D, Chakrabarti OP, Maiti HS, Majumdar R. Si/SiC ceramics from wood of Indian dicotyledonous mango tree. Ceram Int. 2007;33:1217–22.
34. Ueki Y, Yoshiie R, Naruse I, Ohno K, Maeda T, Nishioka K, et al. Reaction behavior during heating biomass materials and iron oxide composites. Fuel. 2013;104:58–61.
35. Moyo M, Emmanuel V, Johannes S. Biosorption of lead (II) by chemically modified *Mangifera indica* seed shells: adsorbent preparation, characterization and performance assessment. Process Saf Environ Prot. 2017;111:40–51.
36. Guo K, Lin L, Fan X, Zhang L, Wei C. Comparison of structural and functional properties of starches from five fruit kernels. Food Chem. 2018;257:75–82.